

Curvaton in light of the ACT results

Christian T. Byrnes,^{1,*} Marina Cortês,^{2,†} and Andrew R. Liddle^{2,‡}

¹*Department of Physics and Astronomy, University of Sussex, Brighton BN1 9QH, UK*

²*Institute of Astrophysics and Space Sciences, Faculty of Sciences, University of Lisbon, 1769-016 Lisbon, Portugal*

(Dated: March 13, 2026)

The latest results from the Atacama Cosmology Telescope Collaboration have moved the preferred perturbation spectral index n_s closer towards one. We reanalyse constraints on the simplest version of the curvaton model, using n_s and the tensor-to-scalar ratio r . We show that in the massless curvaton case the model gives the same locus of n_s - r predictions as the power-law model $V(\phi) \propto \phi^p$, but with a different and more elegant physical interpretation. The model gives an excellent account of current observational data, both in the regime where the curvaton dominates the observed perturbations and with an admixture of inflaton-originated perturbations of up to about one-third of the total. Addition of the newest South Pole Telescope SPT-3G D1 dataset maintains this conclusion in favor of the curvaton model. Forthcoming large-scale structure surveys, such as that of the recently-launched SPHEREx probe, could discriminate between curvaton and single-field inflation models using the bispectrum.

Contents

I. Introduction	1
II. The simplest curvaton model	2
A. Model parameters and density perturbations	2
B. Parametrization of the number of e -foldings	3
C. Observables: Linear power spectrum	3
D. Observables: Non-Gaussianity	5
III. Conclusions	5
Acknowledgements	6
References	6

I. INTRODUCTION

The analysis of cosmological constraints by the Atacama Cosmology Telescope (ACT) collaboration, following their DR6 data release, has indicated a consequential shift upwards in the preferred values of the scalar spectral index n_s , from the *Planck* 2018 value of $n_s = 0.9651 \pm 0.0044$ [1] to $n_s = 0.9743 \pm 0.0034$ [2] (in a compilation using DESI-DR1 data [3–5]). The new central value is just over 2-sigma from the *Planck* result. While within the realm of plausible statistical fluctuations, this change has substantial implications for inflationary modelling. The higher value has been reinforced in subsequent analyses, for example the revised (v2) ACT paper [2] includes an analysis updating to DESI-DR2 [6] that yields the somewhat higher again $n_s = 0.9752 \pm 0.0030$, while the Dark Energy Survey Y6

release finds a yet higher value $n_s = 0.977 \pm 0.003$ from an all-data compilation including *Planck* and ACT [7].

It is worth remarking that only part of the shift comes from the ACT DR6 power spectrum data itself, which combined with *Planck* gives $n_s = 0.9709 \pm 0.0038$ (ACT alone gives quite a wide range for n_s , but the intersection of preferred regions with *Planck* in the full parameter space pulls to the higher values). Only when the ACT and *Planck* power spectra are combined with cosmic microwave background (CMB) lensing and with baryon acoustic oscillation constraints from DESI DR1 [3, 4] does the full shift emerge [2]. Combined with the very strong upper limits on the tensor-to-scalar ratio r coming from BICEP/Keck [8], the viable region of the n_s - r plane is becoming small as well as being displaced from its position of a few years ago.

For instance, those who invested heavily in Starobinsky inflation [9] and its variants [10] following *Planck* now find themselves in the uncomfortable position of only touching the 95% confidence region for a very high pivot e -foldings number of $N_* = 60$ [11],¹ possibly requiring non-standard reheating [13–16]. Another popular option, Higgs inflation [17], has also suffered under this change [14, 18]. Alternatively, rather than seeking to resuscitate models whose favoured status was, after all, to significant extent because they fitted the data that has now shifted, one can construct new models or otherwise modify existing models or theory of gravity to match the current constraints, e.g. Refs. [19–31].

Here we argue that the shift has substantially benefited curvaton models [32–36], including their simplest incarnation using two quadratic potentials [37, 38]. We show that in the usual massless curvaton limit, this model gives

*Electronic address: C.Byrnes@sussex.ac.uk

†Electronic address: mvcortes@ciencias.ulisboa.pt

‡Electronic address: arliddle@ciencias.ulisboa.pt

¹ It is worth remembering that early inflation modelers chose 60 as an estimate for when the present Hubble radius crossed outside during inflation, whereas modern observations are specified at $k_* = 0.05 \text{ Mpc}^{-1}$ which crossed five e -foldings later [12].

the same locus of predictions in the n_s-r plane as the power-law single-field potentials ϕ^p . These are often used as a benchmark in assessing observational constraints, but with an upper limit now well below $p = 1$, this form can be challenging to motivate from fundamental physics considerations (the best-known option is the monodromy models [39, 40], whose most popular value $p = 2/3$ is also now borderline excluded). There is also the question of how to address the non-analyticity at $\phi = 0$. We will argue that the curvaton model provides a compelling alternative explanation of current constraints. This is in sharp contrast to the position after the *Planck* 2018 results [1], where it appeared the curvaton-dominated limit of these models was comfortably excluded (see their Fig. 28) and no model parameters gave a good fit.

II. THE SIMPLEST CURVATON MODEL

A. Model parameters and density perturbations

We restrict our analysis to the simplest curvaton model [37]. This features two massive non-interacting fields with potential

$$V(\phi, \sigma) = \frac{1}{2}m_\phi^2\phi^2 + \frac{1}{2}m_\sigma^2\sigma^2, \quad (1)$$

and a flat field-space metric. The inflaton ϕ is responsible for driving inflation via its potential energy, while the curvaton σ acquires perturbations during inflation that subsequently convert to adiabatic when the curvaton decays to normal matter after inflation ends. We will closely follow the detailed analysis we made in Ref. [38], which allows an arbitrary admixture of inflaton and curvaton contributions to the observed adiabatic power spectrum. A similar recent analysis looking at other choices of the inflaton potential was made in Ref. [41].

The number of e -foldings of inflation from field values ϕ and σ to the end of inflation is given by

$$N = 2\pi \frac{\phi^2 + \sigma^2}{m_{\text{Pl}}^2}, \quad (2)$$

where m_{Pl} is the (non-reduced) Planck mass. By the time observable scales are leaving the horizon, the curvaton field takes a small and effectively constant value σ_* , which is one of the model parameters. Since this value is small compared to m_{Pl} (the inflating curvaton having been observationally excluded [38]) its impact on the above equation is subdominant to the already tiny contribution from the inflaton field value at the end of inflation, which we have also omitted. Sometimes σ_* is estimated using the stochastic prediction for a spectator field in de-Sitter space, which gives $\langle \sigma_*^2 \rangle \sim H_*^4/m_\sigma^2$, but the Hubble parameter varies too rapidly during quadratic inflation for this approach to work [42].

We consider the complete range from negligible to full curvaton contribution to the total power spectrum, given

by

$$\mathcal{P}_\zeta^{\text{total}} = \mathcal{P}_\zeta^\phi + \mathcal{P}_\zeta^\sigma. \quad (3)$$

We can parametrize the inflaton contribution to the total power spectrum as

$$\mathcal{P}_\zeta^\phi = \frac{m_\phi^2}{m_{\text{single}}^2} \mathcal{P}_\zeta^{\text{total}}. \quad (4)$$

Here m_{single} is the mass that the inflaton would need if it were to give the correct amplitude of perturbations in the single-field case; in a scenario where both fields contribute this is an upper limit to the actual inflaton mass m_ϕ . It is determined by

$$\mathcal{P}_{\text{single}} = \frac{8V_{\text{single}}}{3m_{\text{Pl}}^4 \epsilon_{\text{single}}} \Big|_* \quad (5)$$

$$= \frac{4m_{\text{single}}^2 \phi_{\text{single}}^2}{3m_{\text{Pl}}^4} 2N \Big|_*, \quad (6)$$

where $*$ refers to the parameter value when observable scales crossed the Hubble radius during inflation, $V_{\text{single}} = m_{\text{single}}^2 \phi_{\text{single}}^2/2$, and

$$\epsilon_{\text{single}} \equiv \frac{m_{\text{Pl}}^2}{16\pi} \left(\frac{V'}{V} \right)^2 = \frac{1}{2N_*} \quad (7)$$

in the single-field model. Taking the observed amplitude as [2]

$$\mathcal{P}_\zeta^{\text{obs}} \sim 2.1 \times 10^{-9}, \quad (8)$$

we obtain

$$\frac{m_{\text{single}}^2}{m_{\text{Pl}}^2} = 4.9 \times 10^{-9} \frac{1}{N_*^2}. \quad (9)$$

The ratio $f \equiv m_\phi^2/m_{\text{single}}^2$ (with $0 < f \leq 1$)² will appear throughout in our expressions as a measure of the fractional contribution of the inflaton to the total power spectrum in each model.

The curvaton contribution to the power spectrum depends on the ratio of curvaton to background energy density at the time the curvaton decays into the thermal bath:

$$r_{\text{dec}} \equiv \frac{3\rho_\sigma}{4\rho_\gamma + 3\rho_\sigma} \Big|_{\text{decay}}, \quad (10)$$

where we assumed that the inflaton has fully decayed into radiation before the curvaton decays. Equation (10) is defined so as to provide a unified expression for the

² Not to be confused with our previous use of the symbol f as the decay fraction of inflatons to curvatons in Ref. [43].

curvaton perturbation in the regimes of radiation and curvaton domination at the time of decay, which is [44]

$$\mathcal{P}_\zeta^\sigma = \frac{r_{\text{dec}}^2 H_*^2}{9\pi^2 \sigma_*^2}. \quad (11)$$

We use the normalization amplitude Eq. (8) to fix the ratio $r_{\text{dec}}^2 H_*^2 / \sigma_*^2$ and obtain

$$r_{\text{dec}}^2 = 2.8 \times 10^{-7} (1-f) \frac{\sigma_*^2}{m_\phi^2 N_*}, \quad (12)$$

where henceforth N_* is the e -foldings number at which the *Planck* normalization scale 0.05 Mpc^{-1} crosses the Hubble radius during inflation. The required r_{dec} value fixes the decay timescale of the curvaton. Evaluating Eq. (10) requires knowledge of the full curvaton evolution, but in practice we will only use r_{dec} via Eq. (12) as a constraint on model parameters by requiring that it takes the physically realisable values $0 < r_{\text{dec}} < 1$. This also allows a simple generalisation to models where the inflaton decays partly to curvatons which later themselves decay into the thermal bath [43]. We will see that the lower bound is tightened by the constraint on local f_{NL} .

B. Parametrization of the number of e -foldings

To impose accurate constraints we need to identify the correct number of e -foldings corresponding to the $k_* = 0.05 \text{ Mpc}^{-1}$ pivot scale at which observables are evaluated. With V_{hor} the potential when the pivot scale crossed the horizon during inflation, ρ_{end} the energy density at the end of inflation, and ρ_{reh} the energy density at the end of reheating, this is given by [12, 38]

$$N_* = 58 + \frac{1}{4} \ln(rf) + \frac{1}{4} \ln \frac{V_{\text{hor}}}{\rho_{\text{end}}} + \frac{1}{12} \ln \frac{\rho_{\text{reh}}}{\rho_{\text{end}}}, \quad (13)$$

where all quantities are as in single-field models. The factor f is needed because it modifies the normalization of V_{hor} relative to the observed power spectrum amplitude when the curvaton perturbations are non-negligible³, but where we need to include the epoch of curvaton reheating in addition to the usual inflaton reheating. We parametrize the total amount of reheating e -foldings, given by the last term of Eq. (13), as N_{matter} which includes the reheating of both the inflaton and the curvaton, obtaining

$$\frac{1}{12} \ln \frac{\rho_{\text{reh}}}{\rho_{\text{end}}} = -\frac{1}{4} N_{\text{matter}}. \quad (14)$$

For the quadratic inflaton, the middle two terms in Eq. (13) combine into a term which measures the inflaton mass relative to the single-field limit (i.e. those terms cancel in the single-field case), giving

$$N_* = 58 + \frac{1}{4} \ln f - \frac{1}{4} N_{\text{matter}}. \quad (15)$$

We note that this relation sets a firm upper limit of 58 as the number of e -foldings corresponding to the *Planck* pivot scale (see also Ref. [45]).

The appropriate choice of N_* remains a significant uncertainty in inflation modelling [12]. N_{matter} has quite a wide plausible range, for instance $N_{\text{matter}} = 0$ implies instant reheating and no curvaton domination, while positive values allow for both the period of reheating after inflation and any subsequent period of curvaton domination. $N_{\text{matter}} > 16$ would ensure reheating at less than 10^{11} GeV to avoid overproduction of gravitinos, while $N_{\text{matter}} \lesssim 40$ is necessary to ensure reheating before electro-weak symmetry breaking. Reducing the energy scale of inflation is more efficient at reducing N_* and permitting the curvaton to complete reheating before the electroweak scale is reached, whilst allowing circa 15 e -foldings of expansion for the curvaton to dominate after starting with a plausible energy density a million times smaller than the inflaton's leads to $N_* \simeq 38$, showing that even $N_* \lesssim 40$ can be consistent with models of electroweak baryogenesis. Overall, values of N_* in the range 45 to 55 are reasonable, with the lower end corresponding to the usual curvaton-dominated regime and negligible inflaton fluctuations.

C. Observables: Linear power spectrum

We can now make predictions for model observables: the spectral index n_S , tensor-to-scalar ratio r , and non-Gaussianity parameter f_{NL} . The slow-roll parameters are defined by

$$\begin{aligned} \epsilon &= -\frac{\dot{H}}{H^2} \simeq \frac{1}{2} \left(\frac{dV/d\phi}{3H^2} \right)^2; \\ \eta_\phi &= \frac{d^2V/d\phi^2}{3H^2}; \quad \eta_\sigma = \frac{d^2V/d\sigma^2}{3H^2}. \end{aligned} \quad (16)$$

If there is a single period of inflation, $\epsilon \simeq \eta_\phi \simeq 1/2N_*$.⁴

The predicted deviation from scale invariance is [46],

$$n_S - 1 = (1-f)(-2\epsilon + 2\eta_\sigma) + f(-6\epsilon + 2\eta_\phi). \quad (17)$$

This expression allows for ready distinction between the contribution of the inflaton versus curvaton for each model spectrum, as a function of the inflaton contribution f . It reduces to each of these two regimes for $f \sim 1$

³ This factor was omitted in Ref. [38], but the error did not propagate.

⁴ This corrects a typo in Ref. [38], which fortunately was not propagated to any of the results.

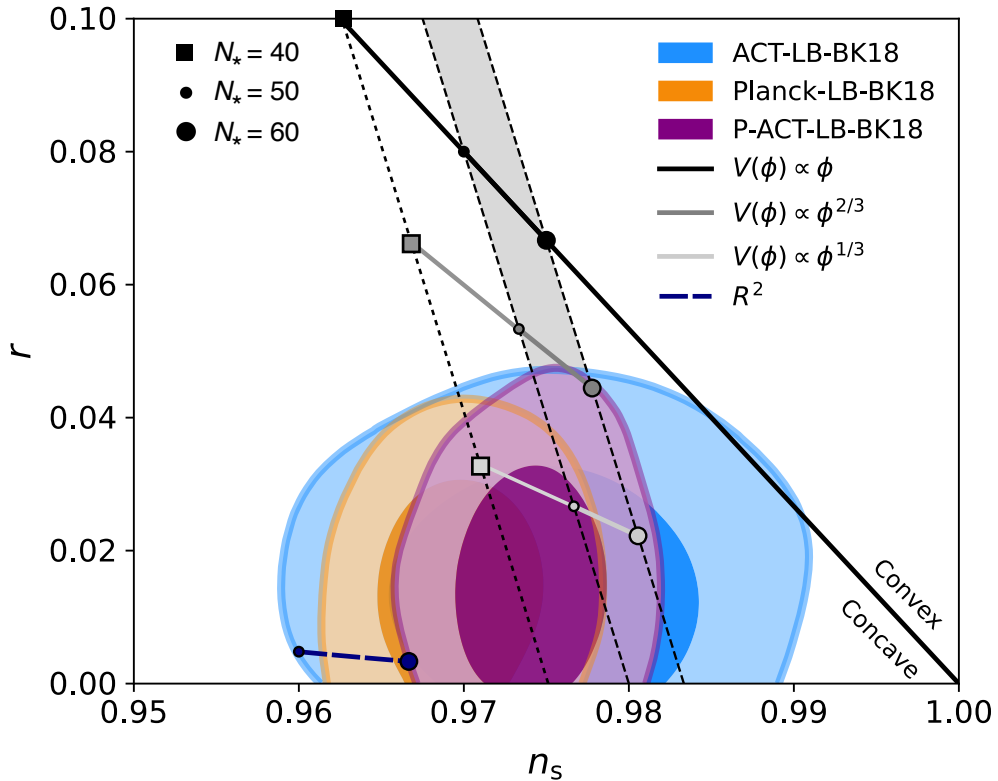


FIG. 1: Observational constraints in the n_s - r plane from Ref. [11]. The combined *Planck*, ACT and BICEP/Keck CMB spectral data, enhanced by CMB lensing and by baryon acoustic oscillation data from DESI-DR1, are shown in purple (see also Figure 59 in v2 of their article for an update to DESI-DR2). The three dashed lines show the power-law potentials for e -folding choices $N_* = 40, 50,$ and 60 , which are also the predictions of our curvaton model in the massless curvaton limit. The sets of symbols, from top to bottom, correspond to $f = 1/2, 1/3,$ and $1/6$. [Adapted from Fig. 10 of Ref. [11], under Creative Commons BY 4.0 License.]

and $f \ll 1$ respectively. We further note that n_s has no dependence on σ_* at leading order in slow-roll. Lastly, Eq. (17) has an implicit dependence on the number of e -foldings and the chosen pivot scale, which we presented in Section II B.

The tensor-to-scalar ratio r is given by [38]

$$r = 16 \epsilon f, \quad (18)$$

also parametrized by the relative contribution of the inflaton mass, and without further dependence on curvaton parameters. As m_ϕ is varied from zero to m_{single} , the prediction in the n_s - r plane interpolates linearly between the curvaton-dominated and inflaton-dominated regimes.

The standard reference guide in discussing observational constraints on inflation is the power-law potential $V(\phi) \propto \phi^p$, whose predictions in the n_s - r plane are seen in Fig. 1 for several N_* values. While early inflation modelling envisaged an even integer power such as $p = 2$ or 4 , observational constraints, particularly the non-detection of r , have now driven the limit on p well below one, making the justification and interpretation of the potential much harder. Even the most-preferred monodromy value of $p = 2/3$ [39, 40] is under strong pressure, especially for

lower N_* values. But remarkably, in the limit of negligible curvaton mass, the curvaton model predicts exactly the same locus in the n_s - r plane, as we now show.

Taking η_σ to be negligible, the curvaton model predictions of Eqs. (17) and (18) simplify to

$$n_s - 1 = -(1+f) \frac{1}{N_*} \quad ; \quad r = \frac{8f}{N_*}. \quad (19)$$

For comparison, a single-field model with $V \propto \phi^p$ gives [47]

$$n_s - 1 = -\left(1 + \frac{p}{2}\right) \frac{1}{N_*} \quad ; \quad r = \frac{4p}{N_*}, \quad (20)$$

which yields the dashed lines shown in Fig. 1. Hence, we have the simple correspondence

$$f \longleftrightarrow \frac{p}{2}. \quad (21)$$

This lets the curvaton model match any p in the range 0 to 2, passing between curvaton and inflaton domination of the generated perturbations respectively. In particular, the curvaton model can exactly mimic the combined

(n_s, r) values of $p < 1$ while using only simple quadratic potentials.

The current observational constraints on r imply $f \lesssim 1/3$ (at 95% confidence), becoming somewhat stronger if N_* is well below 60. Hence, the curvaton perturbations must dominate, but there is still space for a significant (up to 33%) contribution from the inflaton field to the total power spectrum. The curvaton-dominated regime $f \rightarrow 0$, corresponding to $p \rightarrow 0$, gives a good account of the data for the most plausible values of N_* .

Despite the match in the n_s - r predictions, the running of the spectral index will not be identical, as a change in N_* changes the value of m_{single} and hence f .⁵ The runnings $\alpha \equiv dn_s/d\ln k$ for the ϕ^p model [48, 49] and the curvaton model [50] are given, respectively, by

$$\alpha_{\phi^p} = -(n_s - 1)^2 - \frac{r}{8}(n_s - 1), \quad (22)$$

$$\alpha_{\text{curv}} = -(n_s - 1)^2 - \frac{r}{4}(n_s - 1) - \frac{r^2}{32}. \quad (23)$$

Their difference

$$\alpha_{\phi^p} - \alpha_{\text{curv}} = \frac{f(1-f)}{N_*^2}, \quad (24)$$

vanishes in the pure inflaton or pure curvaton limits as expected, and given current limits the difference cannot be larger than $\sim 10^{-4}$, an order of magnitude below the expected sensitivity of near-future experiments [51–53].

If the curvaton mass is non-negligible, n_s is shifted to larger values (greater than unity is even possible); see e.g. Fig. 6 of Ref. [38]. This worsens the data fit, but the observations only limit m_σ to be less than of order m_ϕ which is not very constraining. For example, in the curvaton-dominated limit ($f = 0$), the spectral index is the same if $N_* = 50$ with $\eta_\sigma \ll \eta_\phi$ or if $N_* = 40$ with $\eta_\sigma = \eta_\phi/5$, which corresponds to $m_\sigma \simeq 0.45m_\phi$.

D. Observables: Non-Gaussianity

The curvaton scenario generates non-Gaussianity with the local shape, parametrized by the usual f_{NL} parameter whose value is [44, 54, 55].

$$f_{\text{NL}} = \frac{5}{12} (1-f)^2 \left(\frac{3}{r_{\text{dec}}} - 4 - 2r_{\text{dec}} \right). \quad (25)$$

Note that this expression is independent of the curvaton mass, which does not appear in the expression for r_{dec} . The non-Gaussianity predictions therefore also depend on only two model parameters, but in a plane orthogonal to the two that determine n_s .

In the limit of $m_\phi \ll m_{\text{single}}$ this reduces to the standard curvaton result, while the value is suppressed if the (nearly) Gaussian inflaton perturbations also contribute to the total power spectrum. The limit on f above indicates a maximum suppression of about a factor of $(2/3)^2 \simeq 0.4$.

Taking the *Planck* 95% confidence observational upper limit of $f_{\text{NL}} < 9.3$ [56] leads to $r_{\text{dec}} > 0.11$ in the curvaton limit and $r_{\text{dec}} > 0.05$ if the inflaton contributes 33% of the perturbations. We note that values of r_{dec} quite close to but not equal to one require rather fine-tuned parameters, and hence $r_{\text{dec}} \simeq 1$ should arguably be considered the natural expectation [57, 58]. We therefore expect $f_{\text{NL}} = -5/4$ if the curvaton dominates, a value which SPHEREx, which launched in March 2025, may be able to distinguish from Gaussianity in the next few years [59, 60]. A detection of $f_{\text{NL}} < -5/4$ would completely rule out the quadratic curvaton scenario independently of the inflaton potential, whilst a constraint of e.g. $|f_{\text{NL}}| < 0.5$ would strongly disfavour the curvaton scenario over single-field scenarios which gives rise to $f_{\text{NL}} \simeq 0$. A detection of $f_{\text{NL}} > 0$ would rule out single-field inflation and put tight constraints on r_{dec} . For example if SPHEREx detected $2 < f_{\text{NL}} < 4$ and if constraints on r also significantly strengthened, then this would require $0.21 < r_{\text{dec}} < 0.32$ for the quadratic curvaton scenario to remain viable.

III. CONCLUSIONS

The significant shift in n_s prompted by the ACT DR6 results [2] has restored the viability of simple curvaton models. We have uncovered an exact correspondence between the observational predictions of the simplest curvaton model [37] and the single-field ϕ^p potential that is widely used as a benchmark, with the power-law p replaced by the admixture f of inflaton and curvaton contributions to the perturbations. Moreover, the curvaton model uses only simple quadratic potentials, yet can give predictions that mimic ϕ^p models with $p \ll 1$ that can be otherwise hard to motivate.

The current limit $p \lesssim 2/3$ corresponds to $f \lesssim 1/3$, excluding the inflaton-dominated regime while still permitting a substantial admixture. The curvaton-dominated regime $f \rightarrow 0$ is also a good fit to the data, especially if the e -folding number of the perturbation pivot scale is towards the lower end of our fiducial range $N_* = 45$ to 55. Addition of the newest South Pole Telescope SPT-3G D1 dataset maintains this conclusion in favor of the curvaton model. The data compilation CMB-SPA + DESI (Table VI of Ref. [61]) yields $n_s = 0.9728 \pm 0.0027$, though with some caveats on combining these datasets into a joint analysis.

While we have focused on the simplest implementation of the curvaton scenario [37, 38], clearly other variants can also be expected to give a good fit to current data. Non-Gaussianity provides a challenging but feasi-

⁵ We thank David Wands for pointing this out to us.

ble future route to distinguishing these paradigms from the single-field models.

Acknowledgements

We thank Renata Kallosh and Andrei Linde for comments. Also, we thank Charlotte Wood for pointing out an error in the original version of Eq. (13), and David Wands for important insights concerning the spectral index running. CB is supported by STFC grants ST/X001040/1 and ST/X000796/1. M.C and

A.R.L. were supported by the Fundação para a Ciência e a Tecnologia (FCT) through the research grants UIDB/04434/2020 and UIDP/04434/2020. M.C. acknowledges support from the FCT through the Investigador FCT Contract No. CEECIND/02581/2018 and POPH/FSE (EC), and A.R.L. through the Investigador FCT Contract No. CEECIND/02854/2017 and POPH/FSE (EC). This article/publication is based upon work from COST Action CA21136 – “Addressing observational tensions in cosmology with systematics and fundamental physics (CosmoVerse)”, supported by COST (European Cooperation in Science and Technology).

-
- [1] N. Aghanim et al. (Planck), *Astron. Astrophys.* **641**, A6 (2020), [Erratum: *Astron.Astrophys.* 652, C4 (2021)], arXiv:1807.06209 [astro-ph.CO] .
- [2] T. Louis et al. (Atacama Cosmology Telescope), *The Atacama Cosmology Telescope: DR6 power spectra, likelihoods and Λ CDM parameters* (2025), arXiv:2503.14452 [astro-ph.CO] .
- [3] A. G. Adame et al. (DESI), *JCAP* **04**, 012, arXiv:2404.03000 [astro-ph.CO] .
- [4] A. G. Adame et al. (DESI), *JCAP* **01**, 124, arXiv:2404.03001 [astro-ph.CO] .
- [5] A. G. Adame et al. (DESI), *JCAP* **02**, 021, arXiv:2404.03002 [astro-ph.CO] .
- [6] M. Abdul Karim et al. (DESI), *Phys. Rev. D* **112**, 083515 (2025), arXiv:2503.14738 [astro-ph.CO] .
- [7] T. M. C. Abbott et al. (DES), *Dark Energy Survey Year 6 Results: Cosmological Constraints from Galaxy Clustering and Weak Lensing* (2026), arXiv:2601.14559 [astro-ph.CO] .
- [8] P. A. R. Ade et al. (BICEP, Keck), *Phys. Rev. Lett.* **127**, 151301 (2021), arXiv:2110.00483 [astro-ph.CO] .
- [9] A. A. Starobinsky, *Phys. Lett. B* **91**, 99 (1980).
- [10] R. Kallosh, A. Linde, and D. Roest, *JHEP* **11**, 198, arXiv:1311.0472 [hep-th] .
- [11] E. Calabrese et al. (ACT), *The Atacama Cosmology Telescope: DR6 Constraints on Extended Cosmological Models* (2025), arXiv:2503.14454 [astro-ph.CO] .
- [12] A. R. Liddle and S. M. Leach, *Phys. Rev. D* **68**, 103503 (2003), arXiv:astro-ph/0305263 .
- [13] M. Drees and Y. Xu, *Phys. Lett. B* **867**, 139612 (2025), arXiv:2504.20757 [astro-ph.CO] .
- [14] D. S. Zharov, O. O. Sobol, and S. I. Vilchinskii, *Reheating ACTs on Starobinsky and Higgs inflation* (2025), arXiv:2505.01129 [astro-ph.CO] .
- [15] M. R. Haque, S. Pal, and D. Paul, *ACT DR6 Insights on the Inflationary Attractor models and Reheating* (2025), arXiv:2505.01517 [astro-ph.CO] .
- [16] M. R. Haque, S. Pal, and D. Paul, *Phys. Lett. B* **869**, 139852 (2025), arXiv:2505.04615 [astro-ph.CO] .
- [17] F. L. Bezrukov and M. Shaposhnikov, *Phys. Lett. B* **659**, 703 (2008), arXiv:0710.3755 [hep-th] .
- [18] L. Liu, Z. Yi, and Y. Gong, *Reconciling Higgs Inflation with ACT Observations through Reheating* (2025), arXiv:2505.02407 [astro-ph.CO] .
- [19] R. Kallosh, A. Linde, and D. Roest, *Phys. Rev. Lett.* **135**, 161001 (2025), arXiv:2503.21030 [hep-th] .
- [20] I. D. Gialamas, A. Karam, A. Racioppi, and M. Raidal, *Phys. Rev. D* **112**, 103544 (2025), arXiv:2504.06002 [astro-ph.CO] .
- [21] S. Brahma and J. Calderón-Figueroa, *Is the CMB revealing signs of pre-inflationary physics?* (2025), arXiv:2504.02746 [astro-ph.CO] .
- [22] C. Dioguardi, A. J. Iovino, and A. Racioppi, *Phys. Lett. B* **868**, 139664 (2025), arXiv:2504.02809 [gr-qc] .
- [23] A. Salvio, *Phys. Rev. D* **112**, L061301 (2025), arXiv:2504.10488 [hep-ph] .
- [24] A. Berera, S. Brahma, Z. Qiu, R. O. Ramos, and G. S. Rodrigues, *JCAP* **11**, 059, arXiv:2504.02655 [hep-th] .
- [25] C. Dioguardi and A. Karam, *Palatini Linear Attractors Are Back in ACTion* (2025), arXiv:2504.12937 [gr-qc] .
- [26] M. U. Rehman and Q. Shafi, *Supersymmetric Hybrid Inflation in light of Atacama Cosmology Telescope Data Release 6, Planck 2018 and LB-BK18* (2025), arXiv:2504.14831 [astro-ph.CO] .
- [27] Q. Gao, Y. Gong, Z. Yi, and F. Zhang, *Phys. Dark Univ.* **50**, 102106 (2025), arXiv:2504.15218 [astro-ph.CO] .
- [28] M. He, M. Hong, and K. Mukaida, *JCAP* **09**, 080, arXiv:2504.16069 [astro-ph.CO] .
- [29] W. Yin, *Higgs-like inflation under ACTivated mass* (2025), arXiv:2505.03004 [hep-ph] .
- [30] I. D. Gialamas, T. Katsoulas, and K. Tamvakis, *JCAP* **09**, 060, arXiv:2505.03608 [gr-qc] .
- [31] Yogesh, A. Mohammadi, Q. Wu, and T. Zhu, *Starobinsky like inflation and EGB Gravity in the light of ACT* (2025), arXiv:2505.05363 [astro-ph.CO] .
- [32] S. Mollerach, *Phys. Rev. D* **42**, 313 (1990).
- [33] A. D. Linde and V. F. Mukhanov, *Phys. Rev. D* **56**, R535 (1997), arXiv:astro-ph/9610219 .
- [34] K. Enqvist and M. S. Sloth, *Nucl. Phys. B* **626**, 395 (2002), arXiv:hep-ph/0109214 .
- [35] D. H. Lyth and D. Wands, *Phys. Lett. B* **524**, 5 (2002), arXiv:hep-ph/0110002 .
- [36] T. Moroi and T. Takahashi, *Phys. Lett. B* **522**, 215 (2001), [Erratum: *Phys.Lett.B* 539, 303–303 (2002)], arXiv:hep-ph/0110096 .
- [37] N. Bartolo and A. R. Liddle, *Phys. Rev. D* **65**, 121301 (2002), arXiv:astro-ph/0203076 .
- [38] C. T. Byrnes, M. Cortês, and A. R. Liddle, *Phys. Rev. D* **90**, 023523 (2014), arXiv:1403.4591 [astro-ph.CO] .
- [39] E. Silverstein and A. Westphal, *Phys. Rev. D* **78**, 106003 (2008), arXiv:0803.3085 [hep-th] .
- [40] L. McAllister, E. Silverstein, A. Westphal, and T. Wrase,

- JHEP **09**, 123, arXiv:1405.3652 [hep-th] .
- [41] G. Choi, W. Ke, and K. A. Olive, Phys. Rev. D **111**, 023518 (2025), arXiv:2409.08279 [hep-ph] .
 - [42] R. J. Hardwick, V. Vennin, C. T. Byrnes, J. Torrado, and D. Wands, JCAP **10**, 018, arXiv:1701.06473 [astro-ph.CO] .
 - [43] C. T. Byrnes, M. Cortès, and A. R. Liddle, Phys. Rev. D **94**, 063525 (2016), arXiv:1608.02162 [astro-ph.CO] .
 - [44] D. H. Lyth, C. Ungarelli, and D. Wands, Phys. Rev. D **67**, 023503 (2003), arXiv:astro-ph/0208055 .
 - [45] G. Germán, R. G. Quaglia, and A. M. M. Colorado, JCAP **03**, 004, arXiv:2212.03730 [gr-qc] .
 - [46] D. Wands, N. Bartolo, S. Matarrese, and A. Riotto, Phys. Rev. D **66**, 043520 (2002), arXiv:astro-ph/0205253 .
 - [47] A. R. Liddle and D. H. Lyth, Phys. Lett. B **291**, 391 (1992), arXiv:astro-ph/9208007 .
 - [48] A. Kosowsky and M. S. Turner, Phys. Rev. D **52**, R1739 (1995), arXiv:astro-ph/9504071 .
 - [49] T. Chiba and K. Kohri, PTEP **2014**, 093E01 (2014), arXiv:1406.6117 [astro-ph.CO] .
 - [50] C. T. Byrnes and D. Wands, Phys. Rev. D **74**, 043529 (2006), arXiv:astro-ph/0605679 .
 - [51] D. Schlegel et al. (BigBoss), The BigBOSS Experiment (2011), arXiv:1106.1706 [astro-ph.IM] .
 - [52] K. Kohri, Y. Oyama, T. Sekiguchi, and T. Takahashi, JCAP **10**, 065, arXiv:1303.1688 [astro-ph.CO] .
 - [53] J. B. Muñoz, E. D. Kovetz, A. Raccanelli, M. Kamionkowski, and J. Silk, JCAP **05**, 032, arXiv:1611.05883 [astro-ph.CO] .
 - [54] M. Sasaki, J. Valiviita, and D. Wands, Phys. Rev. D **74**, 103003 (2006), arXiv:astro-ph/0607627 .
 - [55] K. Enqvist and T. Takahashi, JCAP **10**, 034, arXiv:1306.5958 [astro-ph.CO] .
 - [56] Y. Akrami et al. (Planck), Astron. Astrophys. **641**, A9 (2020), arXiv:1905.05697 [astro-ph.CO] .
 - [57] R. J. Hardwick and C. T. Byrnes, JCAP **08**, 010, arXiv:1502.06951 [astro-ph.CO] .
 - [58] J. Torrado, C. T. Byrnes, R. J. Hardwick, V. Vennin, and D. Wands, Phys. Rev. D **98**, 063525 (2018), arXiv:1712.05364 [astro-ph.CO] .
 - [59] O. Doré et al. (SPHEREx), Cosmology with the SPHEREX All-Sky Spectral Survey (2014), arXiv:1412.4872 [astro-ph.CO] .
 - [60] C. Heinrich, O. Dore, and E. Krause, Phys. Rev. D **109**, 123511 (2024), arXiv:2311.13082 [astro-ph.CO] .
 - [61] E. Camphuis et al. (SPT-3G), SPT-3G D1: CMB temperature and polarization power spectra and cosmology from 2019 and 2020 observations of the SPT-3G Main field (2025), arXiv:2506.20707 [astro-ph.CO] .